Available online at www.sciencedirect.com
SCIENCE DIRECT
Thermochimica Acta 447 (2006) 115–120
thermochimica acta
www.elsevier.com/locate/tca

Short communication

Phase and thermal stability of nanocrystalline hydroxyapatite prepared via microwave heating

Siwaporn Meejoo *, Weerakanya Maneeprakorn, Pongtip Winotai

Department of Chemistry, Faculty of Science, Mahidol University, Rama VI Road, Rajathevi, Bangkok 10400, Thailand

Received 20 August 2005; received in revised form 14 April 2006; accepted 18 April 2006
Available online 1 May 2006

Abstract

A simple method to prepare nanocrystalline hydroxyapatite (nHAP) is performed using a precipitation method assisted with microwave heating method. This method can be reported notably with high reproducibility and productivity. The received ceramic powder possesses characteristic of needle-shaped nanocrystals with dimension about 50 nm in diameter and 200 nm in length. The particle size distribution has been confirmed being in the range of 28–159 nm. Thermal analyses revealed that nHAP has at least three thermal events influenced by elevated temperatures. Phase stability and microstructure evolution of the nHAP calcined at temperatures range between 700 and 1200 °C are discussed in terms of the formation of secondary phases, the decomposition of HAP releasing carbonate and water. Various experimental techniques have been employed in this work, including powder X-ray diffraction, IR spectroscopy, DSC and TGA thermal analyses, dynamic light scattering and scanning electron microscopy.

Keywords: Ceramics; Hydroxyapatite; Microwave heating; Nanocrystals; Morphology; Thermal stability; Thermal analyses

1. Introduction

Hydroxyapatite (HAP), the most stable calcium phosphate compound at normal temperatures and the pH between 4 and 12, has the chemical formula, $Ca_{10}(PO_4)_6(OH)_2$, with the Ca/P ratio being 1.67. It is a compound of great interest mostly because its chemical similarity to the mineral component of bones and hard tissues in mammals. The most common form of hydroxyapatite is hexagonal and the crystal structure has been described in the space group $P6_3/m$ with lattice parameters $a = b = 9.422$ Å and $c = 6.883$ Å [1]. However, the stoichiometric HAP has been described as monoclinic, space group $P2_1/b$ with cell parameters $a = 9.4214$ Å, $b = 2a$ and $c = 6.8814$ Å [2,3]. Note that biological apatites are rarely stoichiometric. The major cause of the non-stoichiometry is the incorporation of impurities, often substitutionally for Ca, but also interstitially. In general, the biological compounds are denoted as calcium-deficient (Ca-def), containing a wide variety of relative small amounts of other substitute atoms or groups such as halogen atoms or carbonate ions. HAP can incorporate a wide variety of substitutions for Ca^{2+}, PO_4^{3-}, and/or OH^- ions [4].

Two principle ways of preparing HAP are wet methods [5] and solid-state reactions [6]. Nevertheless, alternative techniques for preparing HAP powders are sol–gel [7], electrocrystallization [8], spray pyrolysis [9], emulsion processing [10], mechanochemical and hydrothermal treatments [11]. Among the different synthesis methods, the chemical precipitation and hydrothermal approach could generate nanocrystalline HAP [12,13], but the former can be carried out at low temperatures and normal pressure. Nevertheless, calcium phosphate precipitation has been described as a fairly complicated process and is known to be dependent on several parameters (stoichiometry, pH, rate of addition, ionic strength, temperature, etc.) [14]. Therefore, it is very important to precisely control the factors governing the precipitation, otherwise small differences of products in stoichiometry, crystallinity, morphology, etc., could contribute to the difference in chemical or clinical behaviors of the calcium phosphate compound [15]. Recently, microwave synthesis of materials offers the advantages of heating throughout the volume and very efficient transformation of energy [16]. Microwave heating is fundamentally different from conventional heating in that the heat is generated internally within the material instead of originating from an external heating and subsequent radiative

* Corresponding author. Tel.: +66 2 201 5164; fax: +66 2 354 7151.
E-mail address: scsmj@mahidol.ac.th (S. Meejoo).

0040-6031/$ – see front matter © 2006 Elsevier B.V. All rights reserved.
doi:10.1016/j.tca.2006.04.013

transfer. In chemistry viewpoint, microwave heating is of higher spatial distribution of heat or transfer rate [17]. In addition, it is a very sensitive function of the material being processed and depends upon such factors as size, geometry, and mass of the sample. In actual practice, the sample in fact becomes the source of heat during microwave processing. From what mentioned above, microwave heating has gained a lot of significance for materials processing mainly because of its intrinsic advantages such as rapid heating rates, reduced processing times, substantial energy savings, and being environmentally cleaner [18]. It is also believed that microwave irradiation could give novel and improved properties, including fine microstructures of products. From this point, if microwave irradiation is introduced in the HAP preparation process, the reaction does not occur via crystallographic transformation; consequently HAP should be precipitated in very small nanosized crystallites.

The principle goals of this research are to synthesize nanocrystalline hydroxyapatite (nHAP) by precipitation method using microwave irradiation and study the nanostructured material in terms of structural information, chemical compositions, microstructures and thermal stability. It has been previously revealed [19] that hydroxyapatite microcrystalline phase could decompose to oxyhydroxyapatite, α-tricalcium phosphate, tetracalcium phosphate, calcium oxide and amorphous apatite at elevated temperature. In this work, a systematic study upon heat treatments on the hydroxyapatite nanocrystals could give an insight of thermal stability of the nanocrystalline phase. Sarig and Kahana [20] reported a method to obtain nanocrystalline hydroxyapatite from a co-precipitation method. By following their instruction, not only very low yield of the precipitate was received but also the process required pH adjustment throughout the reaction. Our research is, additionally, aimed to acquire an alternatively simple instruction that govern the production of nanocrystalline hydroxyapatite with high yield and purity.

2. Experimental

Nanocrystalline HAP (nHAP) was prepared from an aqueous precipitation reaction using 1:1 binary mixture of calcium hydroxide, $Ca(OH)_2$, and diammonium hydrogen orthophosphate, $(NH_4)_2HPO_4$, as Ca and P precursors, respectively. In this study, commercially supplied $Ca(OH)_2$ (99.8% purity) and $(NH_4)_2HPO_4$ (99.8% purity) and de-ionized water were the only starting materials and the reaction can be written as follows:

$$10Ca(OH)_2 + 6(NH_4)_2HPO_4 \rightarrow Ca_{10}(PO_4)_6(OH)_2 + 6H_2O + 12NH_4OH$$

To form a reaction mixture, equivolume of 0.24 M $(NH_4)_2HPO_4$ aqueous solution was slowly added to 0.4 M aqueous suspension of $Ca(OH)_2$ under a constant stirring condition at room temperature. The mixture was then immediately exposed to microwave radiation (850 W) for 20 min and a white paste subsequently formed. Note that the ammonia byproduct was already eliminated from the mixture due to the irradiating heat. Then solvent was completely removed under freeze drying to avoid particle agglomeration. In this freeze-drying process, the frozen slurry was dried by a sublimation of the water component in an iced solution without back melting at 258 K and 0.3 Torr for 6 h. Phase and the chemical constituents of the product were directly characterized by powder X-ray diffraction and IR spectroscopy. Thermal behavior of the as-prepared nHAP powder was determined using differential scanning calorimetry (DSC) and thermogravimetric analyses (TGA). Morphology and particle size distribution of the as-prepared powder were investigated by scanning electron microscopy (SEM) and dynamic light scattering (DLS). The high resolution SEM micrographs displaying the nanometric sized of the as-prepared sample were recorded on a JEOL JSM 6301F scanning microscope, while the others were recorded on a JEOL JSM 6400 microscope, for which energy dispersive spectroscopic (EDS) analysis was performed simultaneously. DLS analysis was carried out on a Mastersizer 2000 Malvern analyzer using de-ionized water as a medium.

Next, three nHAP powder samples were then thermally treated at 700, 800, 900 and 1200 °C in a Lenton model EHF 18/5, furnace in air atmosphere. The heating rate was limited to 4 °C/min until it reached the required temperatures and maintained at those temperatures for 2 h and then cooled down at 5 °C/min back to room temperature.

All powder X-ray diffractograms were recorded on a Bruker AXS D8 Advance powder diffractometer, Cu Kα1 with PSD detector; 2θ range, 25°–45°; step size 0.0154° and step time 1 s. IR spectra were measured on a Perkin-Elmer model PE 2000 FT-IR spectrometer in the wave number region 400–4000 cm^{-1}. All IR measurements were carried out at room temperature using the KBr pellet technique. Both DSC and TGA thermograms were obtained on a DSC–TGA simultaneous thermal analyzer, performing under N_2 atmosphere with a 20 °C/min heating rate over a temperature range between 50 and 1300 °C.

3. Results and discussion

Nanocrystalline hydroxyapatite, nHAP, was successfully prepared via a very simple method. The differences between this method and others are discussed as follows. Firstly, adjusting pH is needless because the $Ca(OH)_2$ suspension is already a strong base. Comparing with other works reported earlier, the mixture of Ca and P precursors must be kept at a pH ≥ 10 throughout the reaction [21]. Secondly, this reaction was carried out in air atmosphere whereas some groups [12] of researcher obtained nanoparticle materials via hydrothermal method for which a relatively high temperature and high-pressure experiment must be operated. Thirdly, it takes only 3 h for the whole process from the step of preparing the precursor solutions, mixing, and microwave heating to finally form the precipitate. The by-product, NH_4OH was readily removed upon evaporation during the heating. This preparation instruction was repeated for five times obtaining identical phase of the nHAP powder characterized as follows.

3.1. Crystalline phases and microstructures

Fig. 1 represents powder diffractograms of the as-prepared nHAP and the nHAP heated at different temperatures. Fig. 1(a) has shown that the as-prepared product is of a single crystalline

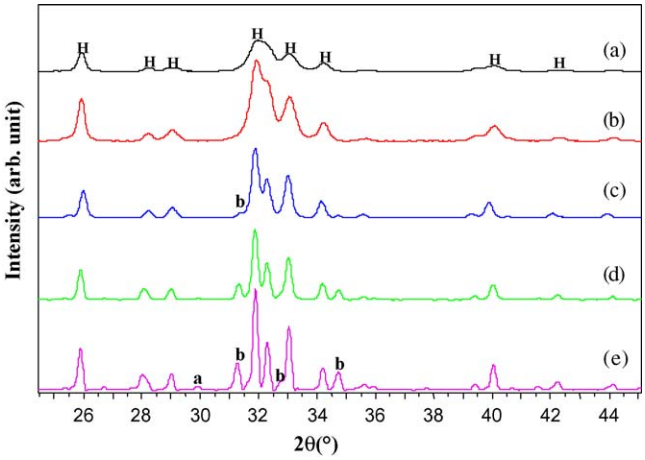

Fig. 1. Powder X-ray diffractograms of the HAP precipitate: (a) as-prepared, (b) calcined at 700 °C, (c) calcined at 800 °C, (d) calcined at 900 °C and (e) calcined at 1200 °C. (H) HAP; (b) β-TCP; (a) α-TCP.

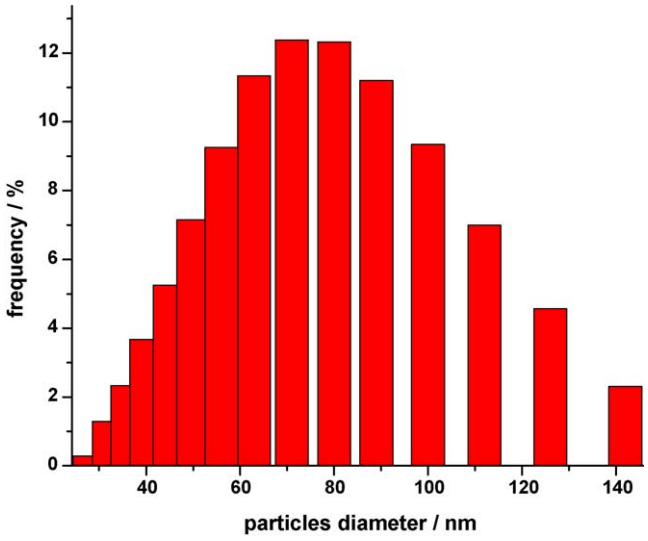

Fig. 3. Histogram representation of the mean diameters of as-prepared nHAP suspended in aqueous solution.

phase of hydroxyapatite (XRD JCPDS data file No. 9-432). The broad, not well resolved diffraction peaks may indicate that either the HAP phase does not perfectly crystallized or the crystals are very tiny. The SEM micrographs of the HAP crystals in Fig. 2 clearly shows nanocrystallites with needle-like structure. The micrographs have confirmed that the broad feature in the diffraction pattern, Fig. 2(a) results from the very tiny particles rather than the poorly crystalline phase. The dimensions of the majority of as-prepared nHAP crystals are about 50 nm in diameter and 200 nm in length. With excellent agreement with the microscopic study, DLS analysis gives an insight that the particle size distribution of the precipitate is in the range of 28–159 nm as shown in Fig. 3.

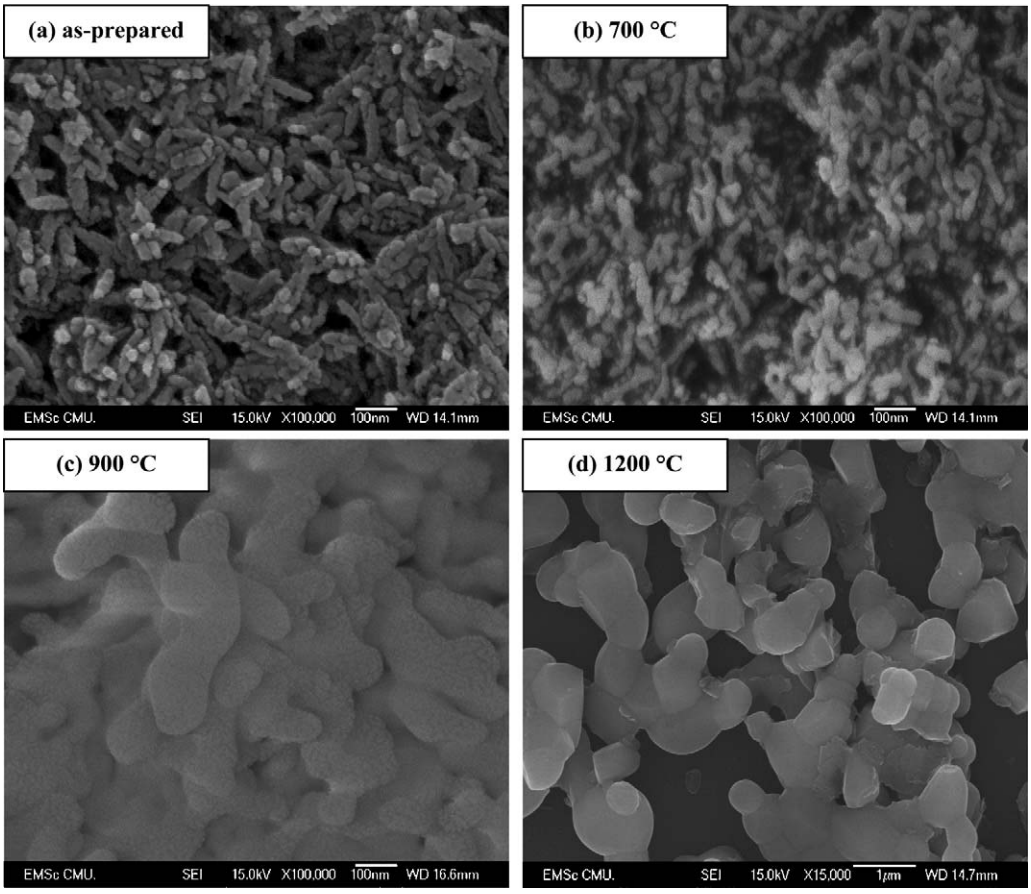

Fig. 2. SEM micrographs of the as-prepared nHAP and the nHAP calcined at temperatures between 700 and 1200 °C.

By heating the nanocrystals, the crystallinity of nHAP increases resulting in the narrowing of diffraction lines as seen in Fig. 1(b)–(e). Upon heat treatment up to 700 °C, the nHAP sample remains stable, as the XRD pattern in Fig. 1(b) only shows an increase in intensity without formation of additional phase. Since the diffraction peaks appear to be slightly broad, the nHAP crystals are expected to be still tiny, but bigger than the parent crystallites. Heating the nanocrystals at 800 °C results better resolved diffraction peaks in Fig. 1(c), indicating the growth of many more crystal planes at high temperature. This involves mass transport to the central growing crystal from the neighboring ones. However, a new diffraction line at 2θ value of 31.1° appeared as a small shoulder on the left side of hydroxyapatite diffraction peaks. The new reflection in Fig. 1(c) is attributed to formation of a fraction of β-TCP due to the decomposition of nHAP. Next, the heat-assisted mass transport experiments performing at 900 and 1200 °C give a significant increase in intensity and resolution for all narrow diffraction peaks. That is the higher of temperature, the narrower of diffraction peaks, and the larger of crystallite sizes. Besides, greater amount of the secondary phase is observed and the powder sample became a mixture of nHAP and β-TCP phase at high temperatures. In comparison to the apatite sample previously reported in literature [21], the decomposition of the reported HAP also occurred at 1000 and 1200 °C. However, the decomposition by-products from the HAP in this work are TCP (α- and β-) whereas those in Ref. [21] are β-TCP and CaO.

The growth and coarsening of crystallites on heating was confirmed by the SEM micrographs of thermally treated nHAP powders. Fig. 2(a) illustrates the particles being held together loosely possibly due to short-range surface forces. These forces may be electrostatic and van der Waal's attractions between particles or liquid capillary forces due to presence of liquid within the granules. It can be concluded from Fig. 2(b) that the grain size of nHAP crystals annealed at 700 °C remains at about 100 nm in diameter, similarly to that of the as-prepared nHAP in Fig. 2(a). It is clear that the grain sizes of nHAP were tripled approximately after annealing at 900 °C as seen in Fig. 2(c). From this point, although the HAP grains are still of nanometric size, it can be seen that the particles joined with their neighbors for the incremental growth process. At higher temperature, 1200 °C, the grain growth process produces a notable increment in grain size of the nHAP sample up to about 1 μm in diameter as shown in Fig. 2(d).

3.2. EDS and IR studies

From EDS analysis, the Ca/P ratio of the as-prepared sample is 1.52, for which two aspects are considered; it may be either tricalcium phosphate (TCP) or calcium deficient HAP. The general formula of non-stoichiometric, calcium deficient (Ca-def) apatite and B-type apatite are $Ca_{10-x}(PO_4)_{6-x}(HPO_4)_x(OH)_{2-x}$ and $Ca_{10-x}(NH_4)_y(PO_4)_{6-x}(CO_3)_x(OH)_2$, respectively, where $(0 \leq x \leq 2)$ [21]. Although they are of apatite structure, the concentration ratio Ca/P, the index for stoichiometry can vary from 1.67 to 1.33. Unfortunately, the theoretical Ca/P atomic ratios of the stoichiometric HAP and TCP are only slightly different and EDS result represents the sample only in a microscopic level. The discrepancy between EDS data and the expected values have been frequently reported with some deviations [22], therefore using EDS is not enough to distinguish HAP and TCP. Infrared spectroscopy is an appropriate method to identify which type of calcium phosphate, HAP or TCP, the sample contains.

All IR spectra in this study were carefully compared with those reported earlier [23,24]. Fig. 4 represents the IR spectrum confirming that the nHAP is of a typical apatite structure. It is common to find substitution formula in the apatite structure and, typically, these could involve carbonate, fluoride and chloride substitutions for either hydroxyl or phosphate groups. From literature [23,24], the characteristic doublet IR peaks around 1450 and 1640 cm^{-1} and the peak at 873 cm^{-1} can be attributed to the vibrational frequencies of carbonate ions substituted at the phosphate site in apatite, so called B-type apatite. Fig. 4(b)–(d) show the IR spectra of the nHAP powders annealed between temperature range of 700–1200 °C. There are significant changes in intensity and appearance of the peaks corresponding to carbonate and hydroxyl groups. It was found that, at 700 °C, the carbonate ions were partially removed from the apatite structure. At 800 °C the powder became the free carbonate form of nHAP. Moreover, at this condition, the condensation process $2HPO_4^{2-}$ to $P_2O_7^{4-}$ takes place resulting a decrease in the intensity of the HPO_4^{2-} band, which extends over the range of 870–840 cm^{-1} together with the presence of a new band

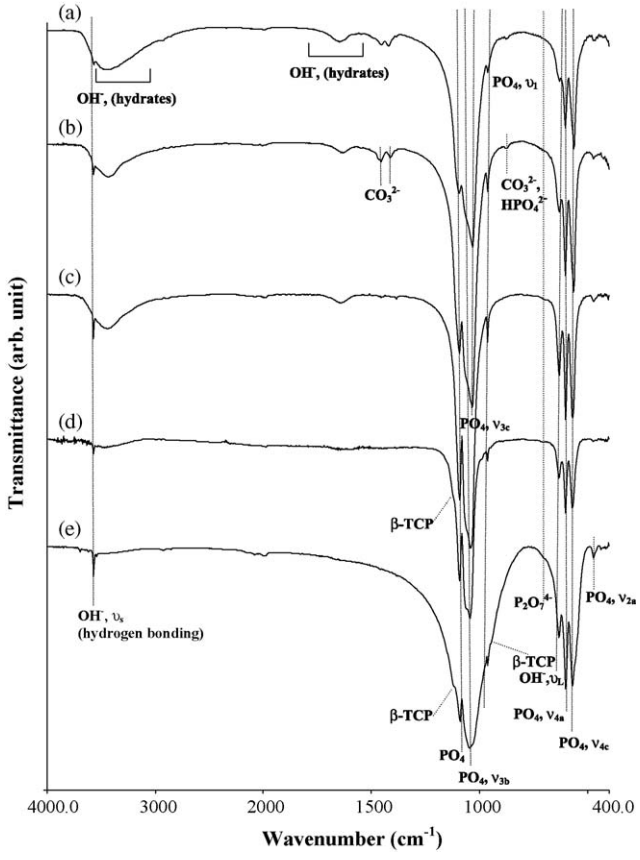

Fig. 4. IR spectra of the HAP precipitates: (a) as-dried, (b) calcined at 700 °C, (c) calcined at 800 °C, (d) calcined at 900 °C and (e) calcined at 1200 °C.

at 715 cm^{-1} assignable to pyrophosphate groups [24]. Furthermore, it is important to point out that the OH^- absorption bands were also affected by the elevated temperatures. The OH^- peaks, at about 3500 cm^{-1}, become narrower at 700 °C, indicating the removal of some amount of hydroxyl component such as water from the crystalline structure. After heat treatment at 900 °C, the OH^- absorption band disappeared and the spectrum, Fig. 4(d), IR spectrum contains some feature according to β-TCP minor phase, observed from the band shoulders around 947, 974 and 1120 cm^{-1} [23]. As shown in Fig. 4(e), the characteristic peaks of β-TCP can be detected more obviously for the nHAP sample calcined at 1200 °C, along with changes of the positions of the PO_4^{3-} vibration bands at 603 and 565 cm^{-1} to 601 and 571 cm^{-1}, as well as at 1094 and 1032 cm^{-1} to new positions at 1090 and 1046 cm^{-1}, respectively. This stands to a reason that phosphate also thermally decomposed.

3.3. Thermal analyses

Fig. 5 illustrates thermogravimetric analysis (TGA) and differential scanning calorimetric (DSC) measurement of the as-prepared nHAP sample. Mass losses in TGA plot represent thermal stability of the sample and may also represent chemical decomposition or vaporization and sublimation at higher temperatures. On heating up to ca. 620 °C, a mass loss of 6.5% is observed from total mass loss of 8.5% of this material. This change of mass could be attributed to the partial removal of physically and chemically adsorbed water and possibly lattice water. This consistent with the IR results where the OH^- band at 3500 cm^{-1} is narrower at elevated temperatures. According to the IR spectrum of the nHAP sample calcined at 800 °C, Fig. 4(c), a mass loss between the temperature range of 600–900 °C possibly corresponds to the decarboxylation of the HAP, releasing CO_2(g) and the condensation of HPO_4^{2-} releasing water. The carbonate bands completely disappear after heating at 800 °C. Note that this decomposition process is concurrent with the dehydroxylation of the nHAP sample, as the intensity of IR absorption bands corresponding to water reduce significantly after heating at 900 °C. In this study, the DSC measurement was carried out to investigate endo- or exothermic reaction or possible phase transitions of the HAP sample. Despite broad features, the DSC traces have revealed three endothermic peaks at 100, 842, and 1104 °C, for which all are related to the changes in mass of the material. According to the TGA traces and IR spectra, the first endothermic peak could be assigned to desorption of adsorbed water, and further heating up to 600 °C possibly brings about the elimination of interstitial water in crystal lattice. Considering the thermograms and the diffraction patterns of nHAP at high temperatures, the second endothermic behavior may represent the decarboxylation together with dehydroxylation of the HAP sample, as well as the decomposition of HAP to β-TCP, whereas the last one involves the decomposition of HAP to β-TCP and α-TCP phases.

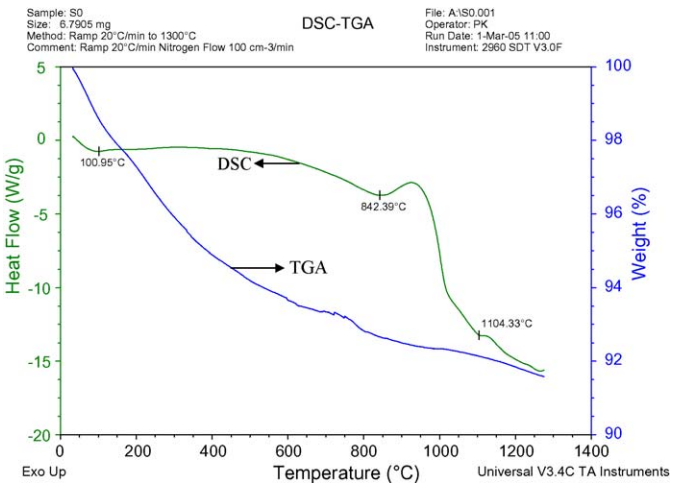

Fig. 5. DSC and TGA plot of the as-prepared nHAP.

Note that calcium deficient apatite and carbonated hydroxyapatite tend to decompose to stoichiometric HAP and TCP at the temperature below 700 °C. Tampieri et al. [25] found that the addition of $Ca(OH)_2$ to calcium deficient apatite can compensate the off-stoichiometry and produce a positive effect in terms of promoting phase stability at high temperatures. This observation is consistent with our work such that the nanocrystalline hydroxyapatite prepared in this work is thermally stable up to 800 °C.

4. Conclusions

A simple, high yield process involving inexpensive reagents, no control of pH and no by-products, has been set up for the production of nanocrystalline hydroxyapatite. The nHAP powder obtained by the present method shows needle shaped crystals with dimension 50 nm × 200 nm. The as-prepared is calcium deficient hydroxyapatite with substitution of CO_3^{2-} for PO_4^{3-} sites, termed B-type carbonate HAP. However, carbonate can be perfectly removed after annealing at 800 °C, but the secondary phases, β-TCP and α-TCP, also formed after heating nHAP at 900 °C or above. DSC and TGA thermograms give consistent results with diffraction and IR studies, for which the thermal transformation of nHAP involved to dehydroxylation and decarboxylation and phosphate decomposition. The nanometric grain size of HAP seemed to be thermally stable up to 900 °C, and changed to the size in micrometer at 1200 °C.

Acknowledgements

This research was financially supported from Thailand Research Fund (Grant #MRG4780077) and Postgraduate Education and Research Program in Chemistry (Perch-ADB).

References

[1] R.A. Young, J.C. Elliott, Arch. Oral Biol. 11 (1966) 699–707.
[2] J.C. Elliot, Structure and Chemistry of the Apatites and Other Calcium Orthophosphates, volume 18 of Studies in Inorganic Chemistry, Elsevier Science B.V., 1994.
[3] J.C. Elliott, P.E. Mackie, R.A. Young, Science 180 (1973) 1055–1057.
[4] A.P. Shpak, V.L. Karbovskii, A.G. Vakh, J. Electron Spectrosc. 137–140 (2004) 585–589.
[5] C. Liu, Y. Huang, W. Shen, J. Cui, Biomaterials 22 (2001) 301–306.

[6] X. Yang, Z. Wang, J. Mater. Chem. 8 (1998) 2233–2237.
[7] W. Feng, L. Mu-sen, L. Yu-peng, Q. Yong-xin, Mater. Lett. 59 (2005) 916–919.
[8] S.K. Yen, C.M. Lin, Mater. Chem. Phys. 77 (2003) 70–76.
[9] K. Itatani, T. Nishioka, S. Seike, F.S. Howell, A. Kishioka, M. Kinoshita, J. Am. Ceram. Soc. 77 (1994) 801–805.
[10] C.-W. Chen, R.E. Riman, K.S. TenHuisen, K. Brown, J. Cryst. Growth 270 (2004) 615–623.
[11] G.Z. Hui, Z. Qingshan, H.X. Zhao, Mater. Res. Bull. 40 (8) (2005) 1326–1334.
[12] W.L. Suchanek, K. Byrappa, P. Shuk, R.E. Riman, V.F. Janas, K.S. TenHuisen, J. Solid State Chem. 177 (2004) 793–799.
[13] R.E. Riman, W.L. Suchanek, K. Byrappa, C.-W. Chen, P.l. Shuk, C.S. Oakes, Solid State Ionics 151 (2002) 393–402.
[14] P.N. Kumta, C. Sfeir, D.-H. Lee, D. Olton, D. Choi, Acta Biomater. 1 (2005) 65–83.
[15] R. Kumar, K.H. Prakash, P. Cheang, K.A. Khor, Langmuir 20 (13) (2004) 5196–5200.
[16] P. Parhi, A. Ramanan, A.R. Ray, Mater. Lett. 58 (2004) 3610–3612.
[17] A. Harrison, A.G. Whittaker, Comprehensive Coordination Chemistry II, 2004, Chap. 1.42, pp. 741–745.
[18] D.A. Jones, T.P. Lelyveld, S.D. Mavrofidis, S.W. Kingman, N.J. Miles, Resour. Conserv. Recycl. 34 (2) (2002) 75–90.
[19] C.-J. Liao, F.-H. Lin, K.-S. Chen, J.-S. Sun, Biomaterials 20 (19) (1999) 1807–1813.
[20] S. Sarig, F. Kahana, J. Cryst. Growth 237–239 (2002) 55–59.
[21] Z. Yang, Y. Jiang, Y. Wang, L. Ma, F. Li, Mater. Lett. 58 (2004) 3586–3590.
[22] K. Kieswetter, T.W. Bauer, S.A. Brown, F. Van Lente, K. Merritt, Biomaterials 15 (1994) 183–188.
[23] I. Manjubala, M. Sivakimar, Mater. Chem. Phys. 71 (2001) 272–278.
[24] A. Ito, S. Nakamura, H. Aoki, M. Akao, K. Teraoka, S. Tsutsumi, K. Onuma, T. Tateishi, J. Cryst. Growth 163 (3) (1996) 311–317.
[25] A. Tampieri, G. Celotti, S. Sprio, C. Mingazzini, Mater. Chem. Phys. 64 (1) (2000) 54–61.